

## Background

Urothelial carcinoma is fairly common, with an estimated 74,000 new cases diagnosed, representing approximately 4.5% of all new cancer cases in the United States in 2015.<sup>1</sup> In patients with metastatic disease an important prognostic factor includes the presence of visceral metastasis (e.g. lung, liver, bone).<sup>2</sup> Treatment options for metastatic disease are limited to systemic therapies, such as cabozantinib chemotherapy. Cabozantinib works by inhibiting the tyrosine kinase activity of MET, VEGFR, c-KIT, and RET.<sup>3</sup>

Patterns of metastasis have been studied in various cancer types by means radiologic imaging, and less frequently by autopsy reviews through population-based analysis and small retrospective analysis.<sup>4-8</sup> Computed tomography (CT) scans, magnetic resonance imaging, and bone scans are commonly used throughout the care and maintenance of urothelial carcinoma. However, there is an underwhelming amount of data/research that utilizes radiologic imaging as a tool to assess metastatic patterns. We seek to address this gap by introducing a heatmap, created by CT image data, as a tool to visualize the patterns of metastases in patients with urothelial cancer.

## Objectives

1. To explore the use of tumor volume-derived heatmaps as a tool to visualize patterns of metastasis in patients with urothelial carcinoma treated with cabozantinib
2. To assess differences in the patterns of metastases among men and women
3. Present changes in volume-derived metastatic distributions in patients who have progressed or responded based on standard radiologic assessment after cabozantinib therapy

## Methods and Materials

**Volumetric lesion images:** Were created in the Picture Archiving Communication System (PACS)<sup>9</sup> from volumetric segmentations of 576 metastatic lesions on CT scans in 45 patients with urothelial carcinoma, enrolled in a phase II trial of single-agent cabozantinib.

**Heatmaps:** Three-dimensional (3D) MultiPlanar Volume Rendering (MPVR) algorithms within PACS were applied to capture skin images for all patients and to highlight segmented volumetric lesion metastasis as discrete objects, all captured in the anterior plane.

All images were linearly transformed to a standard mean size, and then the integrated binary lesion segmentations were overlaid on integrated binary skin images for orientation.

As overlapping frequency increased across patients, a color gradient (heatmap) was created using Matlab<sup>®</sup> with accompanying colormap intensity scales representing data frequency.

**Treatment response assessment:** Representative volumetric tumor lesion images, of a few example patients at time of best response and at progression, were also captured in the anterior plane of the 3D MPVR post-processing algorithm.

## Patient Baseline Characteristics

(N=45 or *N=44)					
	n	%		n	%
Age median (min, max)	63 (41,82)		Primary Site*	Bladder	26 59
				Upper Tract	15 34
Gender	male	30 67	Other	3 7	
	female	15 33		Lymph nodes	33 73
# of Prior Therapies*	1	15 35	Lung	17 38	
	2	18 41	Liver	9 20	
	3	6 14	Bladder	7 16	
	4	2 4	Kidney	4 9	
	5	1 2	Adrenal gland	3 7	
	6	2 4	Other	12 27	

Table I. Demographic information table of 45 patients with urothelial cancer at baseline

## Results

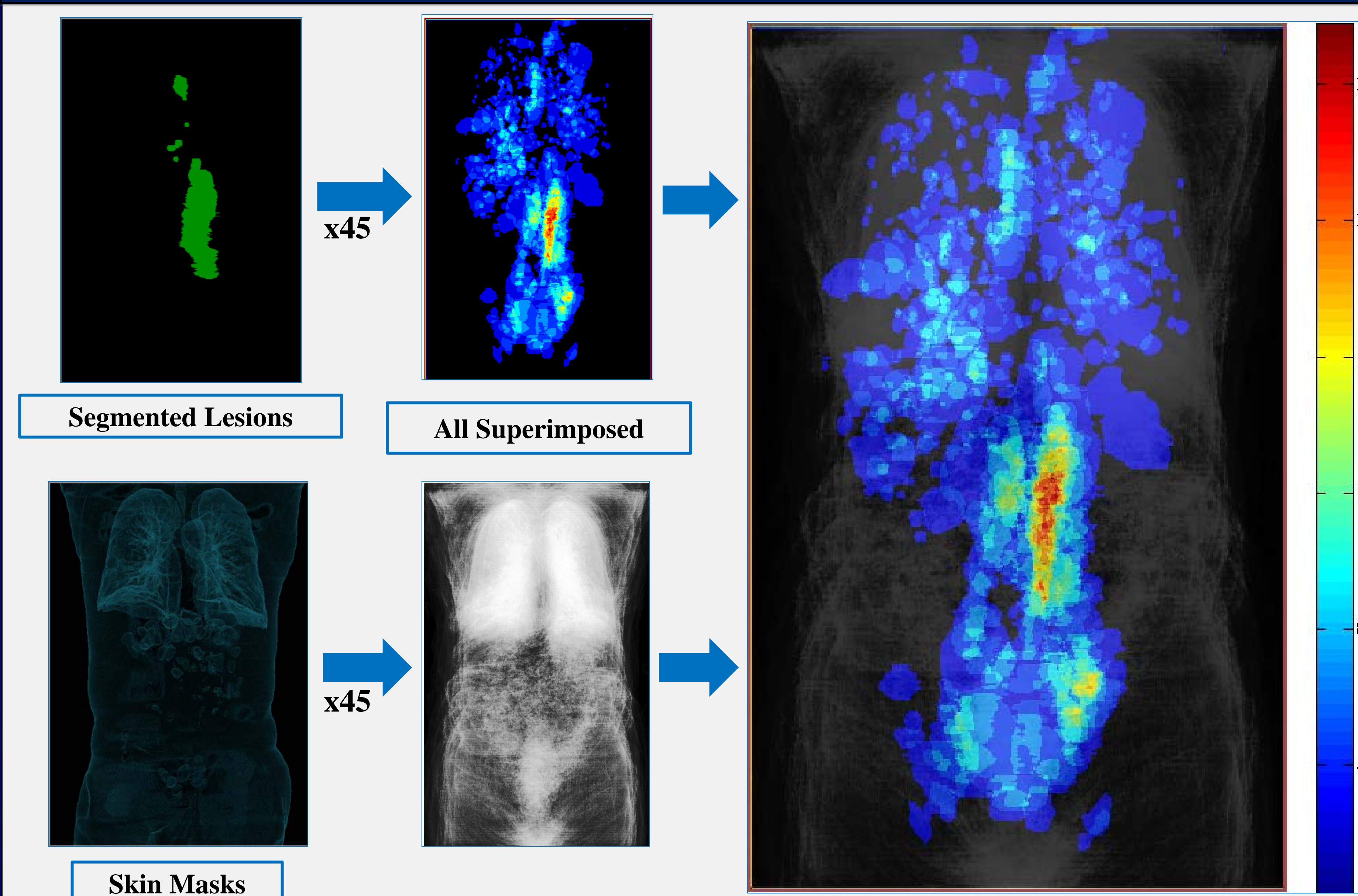


Figure I. Heatmap of all urothelial metastatic lesions in 45 patients, superimposed, demonstrating increased frequency of left-sided retroperitoneal and pelvic lymphatic spread.

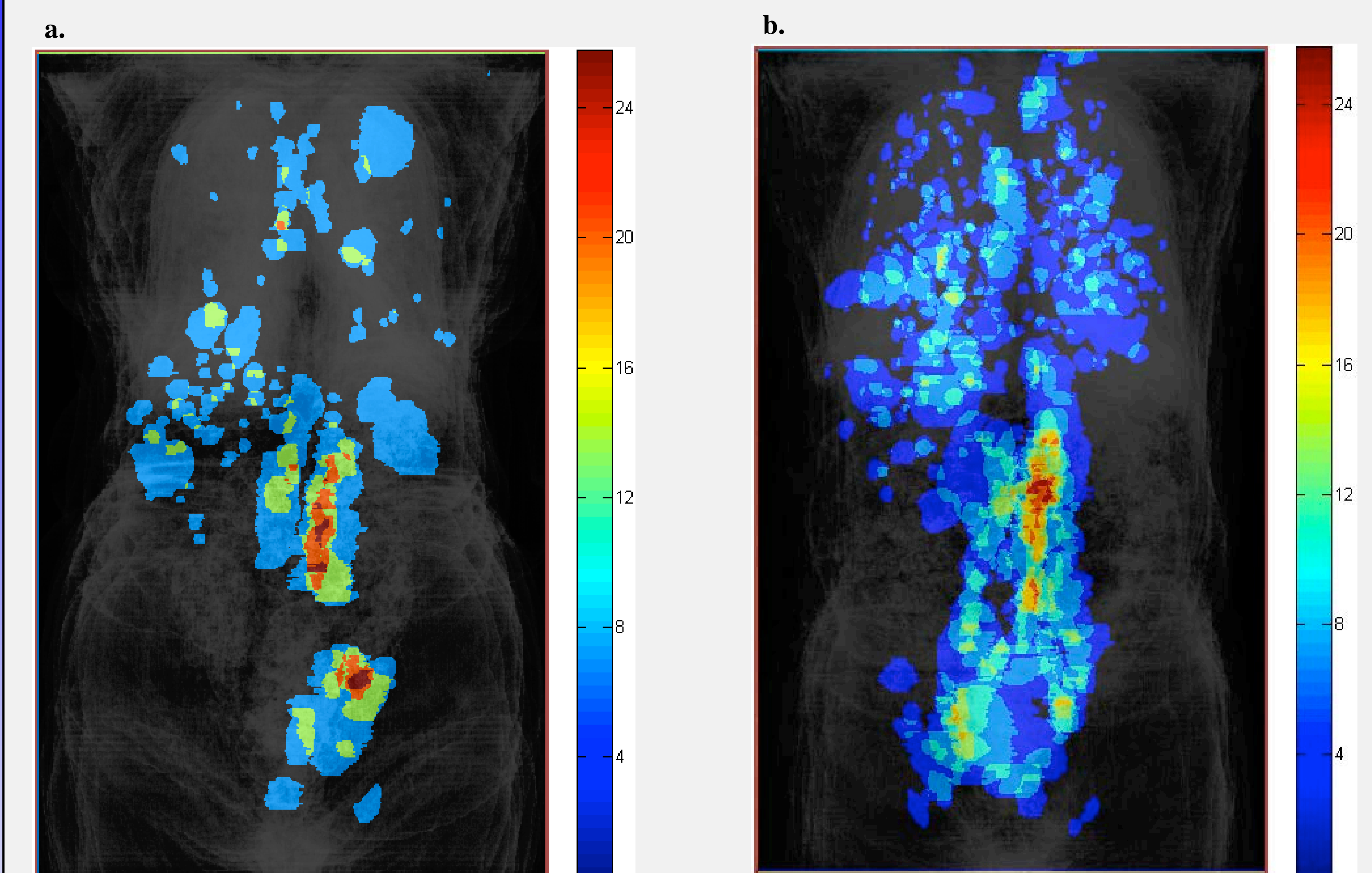


Figure II. Heatmaps of all urothelial metastatic lesions in this representative sample of 15 women (a) and 30 men (b) show broader lungs metastases distribution in men, increased frequency of left sided pelvic adenopathy in women, and both show increased frequency of left-sided retroperitoneal adenopathy.

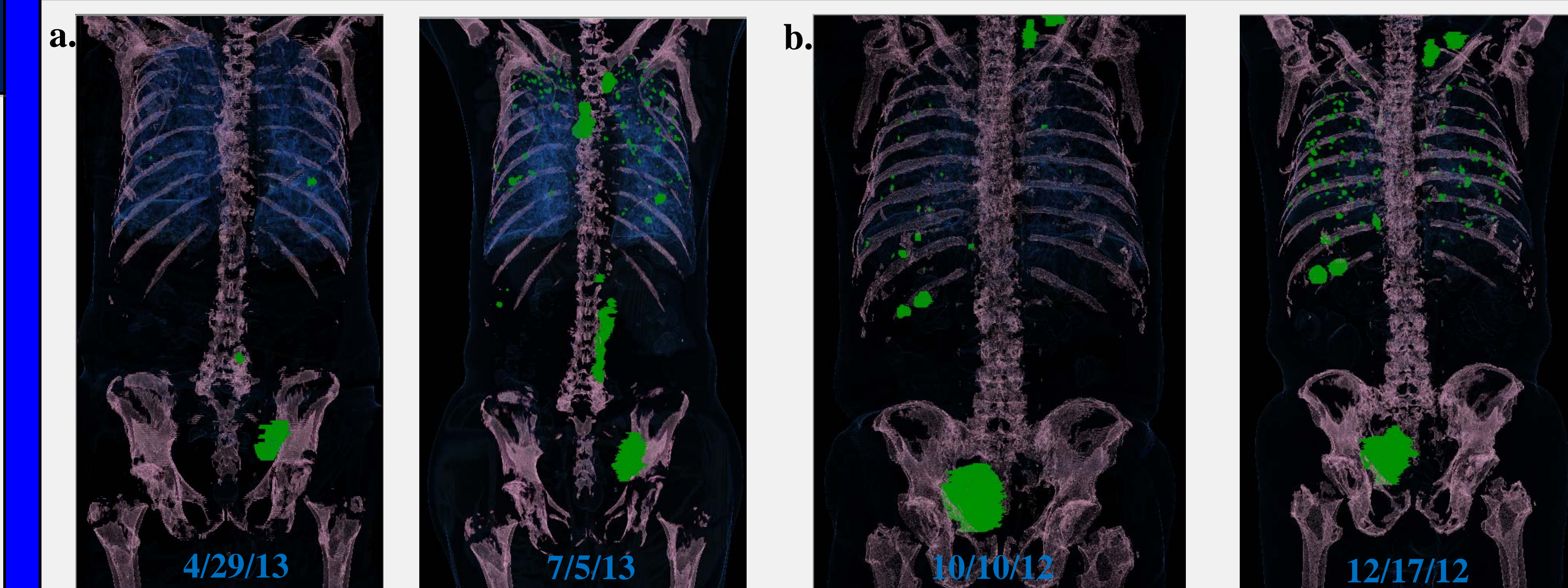


Figure III. Patients with metastatic urothelial carcinoma who show progression from baseline to the 1<sup>st</sup> follow-up. Increased lung metastasis in both cases (a,b), and growth of left retroperitoneal and pelvic lymph nodes (a)

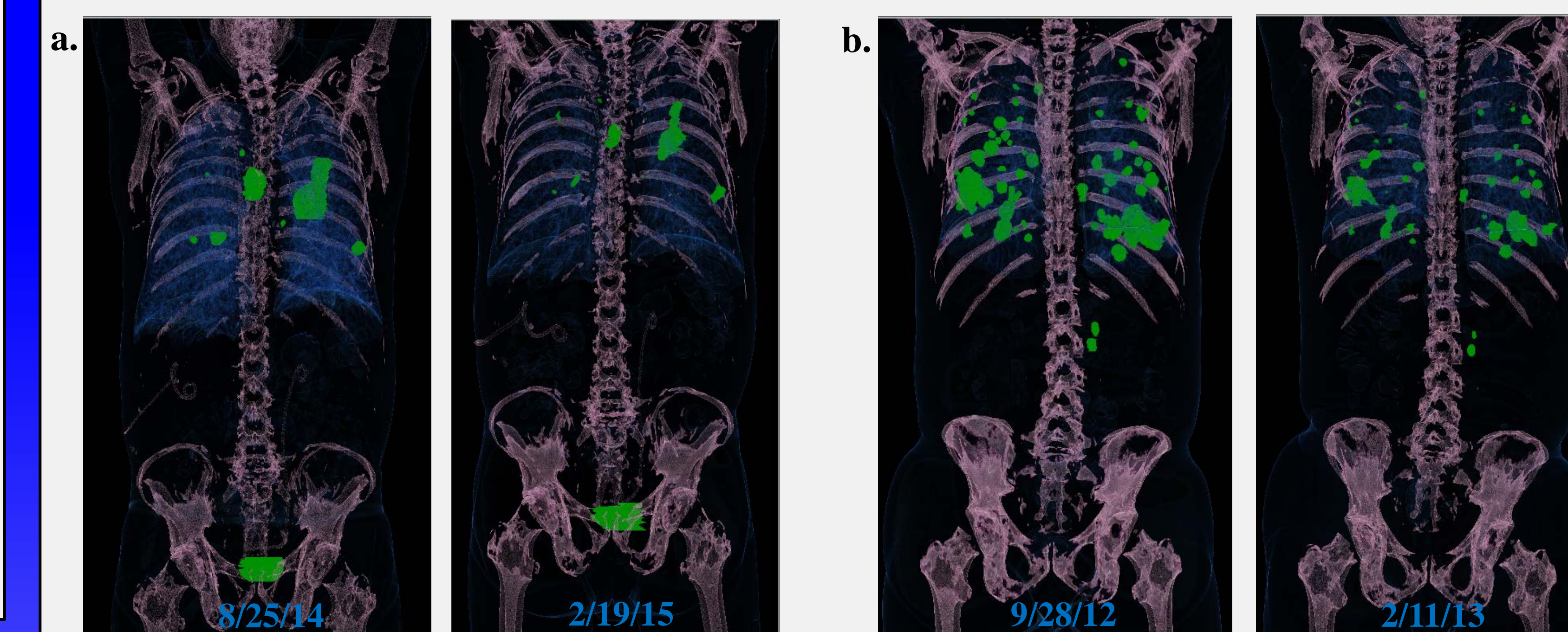


Figure IV. Patients with metastatic urothelial carcinoma who responded to cabozantinib treatment with a 38% (a) and 33% (b) reduction of the target lesions by RECIST.

## Conclusions

The heatmap calculations show that within our cohort of patients with urothelial carcinoma, the distribution of retroperitoneal and pelvic lymphadenopathy is more frequent on the left.

Preliminarily, there appears to be differences in the pattern of metastasis in males versus females; both primarily localized to the left retroperitoneal, however, female patients have more left pelvic metastases.

## Discussion and Clinical Relevance

Metastatic lesion distributions often have predictable patterns depending on the primary cancer. Our heatmaps highlight distribution frequency in one cohort of patients with urothelial cancer.

Similar maps and atlases may help assess metastasis and predict prognosis of patients with metastatic disease using probability models developed by heatmaps of actual patients with certain primary cancers.

Heatmaps may also assist oncologists and radiologists understand various cancer distributions with convenient references and comparisons.

## References

1. Surveillance, Epidemiology, and End Results Program Turning Cancer Data Into Discovery. (n.d.) Retrieved July 14, 2015.
2. Andrea, A., & William, D. (2014). Bladder Cancer. In *The Bethesda Handbook of Clinical Oncology* (Fourth ed., pp. 208-217). Philadelphia: Wolters Kluwers Health.
3. Lindsay, S., & Thomas, H. (2014). Anticancer Agents. In *The Bethesda Handbook of Clinical Oncology* (Fourth ed., pp. 595-596). Philadelphia: Wolters Kluwers Health.
4. Gandaglia, G., Abdollah, F., Schiffman, J., & Trudeau, V. (2013). Distribution of metastatic sites in patients with prostate cancer: A population-based analysis. *Prostate*, 74(2), 210-216. doi:10.1002/pros.22742
5. Bianchi, M., Roghmann, F., Becker, A., Sukumar, S., Briganti, A., Menon, M., ... Trinh, Q.-D. (2014). Age-stratified distribution of metastatic sites in bladder cancer: A population-based analysis. *Canadian Urological Association Journal*, 8(3-4), E148-E158. doi:10.5489/cuaj.787
6. Kasuya, G., Toita, T., Furutani, K., Kodaira, T., Ohno, T., Kaneyasu, Y., ... Hiraoka, M. (2013). Distribution patterns of metastatic pelvic lymph nodes assessed by CT/MRI in patients with uterine cervical cancer. *Radiation Oncology (London, England)*, 8, 139. doi:10.1186/1748-717X-8-139
7. Shinagare, A., Ramani, N., Jagannathan, J., & Fennessey, F. (2011). Metastatic Pattern of Bladder Cancer: Correlation With the Characteristics of the Primary Tumor. *American Journal of Roentgenology*, 196(1), 117-122. doi:10.2214/AJR.10.5036
8. Budczies, J., M. von Winterfeld, F. Klauschen, M. Bockmayr, J. K. Lennerz, C. Denkert, T. Wolf, et al. 2015. The landscape of metastatic progression patterns across major human cancers. *Oncotarget* 6 (1): 570-583.
9. Carestream 12.0. Rochester, New York
10. MathWorks, Natick, Massachusetts